

## SAR and X-ray. A New Approach Combining Fragment-Based Screening and Rational Drug Design: Application to the Discovery of Nanomolar Inhibitors of Src SH2

Dominique Lesuisse,<sup>\*,†</sup> Gudrun Lange,<sup>‡</sup> Pierre Deprez,<sup>†</sup> Didier Bénard,<sup>†</sup> Bernard Schoot,<sup>§</sup> Georges Delettre,<sup>†</sup> Jean-Pierre Marquette,<sup>§</sup> Pierre Broto,<sup>†</sup> Véronique Jean-Baptiste,<sup>||</sup> Paulette Bichet,<sup>§</sup> Edoardo Sarubbi,<sup>§</sup> and Eliane Mandine<sup>||</sup>

Medicinal Chemistry, Central Research, Bone Disease Domain, Aventis, 102 Route de Noisy, F-93235 Romainville Cedex, France, and Structural Biology, Aventis, 65926 Frankfurt, Germany

Received May 15, 2001

pp60Src is a protein involved in signal transduction and is mainly expressed in neurones, platelets, and osteoclasts. Its precise biological role was recently discovered with the KO experiments by Soriano that gave rise to no other apparent phenotype than osteopetrosis, a disease resulting in excedent bone formation. The SH2 domain of the Src family specifically recognizes a sequence of tetrapeptide featuring a phosphotyrosine and a lipophilic amino acid at the +1 and +3 positions. Recently we engaged in the search for SH2 ligands via modular peptidomimicry of this tetrapeptide. This gave rise to several families of nanomolar inhibitors; the best one incorporated a caprolactam scaffold, a biphenyl moiety, and a phosphotyrosine. However, these inhibitors still incorporated the phosphate group that confers good binding affinity to the protein. Phosphates have undesirable features for drug candidates, namely, high rate of hydrolysis of the phosphate group by phosphatases and high charge content precluding cell penetration. Therefore, while searching for optimal non-peptide ligands for Src SH2, we looked for phosphate replacements. For this, we have designed an SAR by fragment crystallography approach. The start of this work resulted from two experimental observations. First, the fact that phenyl phosphate itself displayed detectable binding affinity for Src SH2 permitted us to perform a screening of small aromatic compounds as phenyl phosphate surrogates. Second, the obtention of large Src SH2 crystals displaying a channel large enough for soaking purposes allowed structure determination of over 40 of these small aromatic compounds bound in the phosphotyrosine binding pocket. This search and the way it gave rise to low nanomolar range Src SH2 inhibitors devoid of phosphate groups will be the subject of the present paper.

### Introduction

pp60Src is a protein involved in signal transduction, which is mainly expressed in neurones, platelets, and osteoclasts.<sup>1</sup> Its precise biological role was recently discovered during KO experiments by Soriano<sup>2</sup> that gave rise to no other apparent phenotype than osteopetrosis, a disease resulting in excedent bone formation. This experiment strongly supported an essential role for Src in bone resorption<sup>3</sup> and suggested that a compound capable of inhibiting this protein should inhibit bone resorption and could be useful for the treatment of osteoporosis.

Src is a member of the family of 10 homologous proteins featuring several functional domains, including a tyrosine kinase catalytic domain and SH2<sup>4</sup> and SH3<sup>5</sup> domains involved in protein–protein interactions. Rescue experiments<sup>6</sup> suggested that the SH2 domain is

critical to the bone-resorbing activity of Src, and therefore, we embarked on a program of finding inhibitors of the SH2 domain of Src.

The SH2 domain of the Src family specifically recognizes a tetrapeptide sequence featuring a phosphotyrosine and a lipophilic amino acid at the +1 and +3 positions, respectively.<sup>7</sup> In particular pYEEI, a sequence found on the PDGF receptor upon activation,<sup>8</sup> has been shown to specifically recognize the Src SH2 domain. The approach that we have used to discover non-peptidic inhibitors of this tetrapeptide sequence has been rational-drug-design-driven and has led rapidly to nanomolar range inhibitors of Src SH2. These new inhibitors were derived from a peptidomimetic modular approach where the pYEEI peptide was viewed as a three-component ligand (phosphotyrosine–scaffold–hydrophobic). The tightest ligand that we have identified from this research incorporated a caprolactam spacer,<sup>9</sup> a biphenyl hydrophobic moiety, and a phosphotyrosine. It demonstrated an IC<sub>50</sub> of 9 nM in our Src SH2 scintillation proximity binding assay (SPA)<sup>10</sup> (pYEEINH<sub>2</sub>, 150 nM in the same assay). This inhibitor was crystallized with Src SH2 and was shown to be in perfect alignment with pYEEINH<sub>2</sub>.<sup>9</sup>

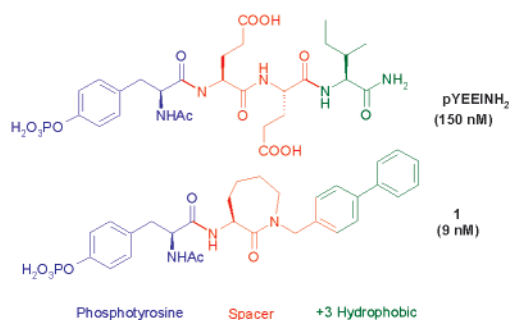
\* To whom correspondence should be addressed. Phone: +33-1-49915341. Fax: +33-1-49915087. E-mail: dominique.lesuisse@aventis.com.

<sup>†</sup> Medicinal Chemistry.

<sup>‡</sup> Structural Biology.

<sup>§</sup> Central Research.

<sup>||</sup> Bone Disease Domain.



However, these inhibitors still incorporated the phosphate group that confers good binding affinity to the protein. Phosphates have undesirable features for drug candidates, namely, high rate of hydrolysis of the phosphate group by phosphatases<sup>11</sup> and high charge content, which precluded cell penetration.<sup>12</sup> Therefore, while searching for optimal non-peptide phosphate ligands for Src SH2, we looked for phosphate replacements. This search and the way it gave rise to low nanomolar range Src SH2 inhibitors lacking phosphate groups will be the subject of the present paper.

## Results and Discussion

The starting point of this work resulted from two experimental observations. First is the fact that phenyl phosphate itself displayed detectable binding affinity for Src SH2. We routinely used two binding assays:<sup>10b</sup> surface plasmon resonance (SPR)<sup>13</sup> and SPA.<sup>10</sup> Affinities of phenyl phosphate and pYEEINH<sub>2</sub> for Src SH2 are compared in Table 1. That such a small fragment gave detectable binding affinity led us to hypothesize that we could engage in a search for nonhydrolyzable phosphate mimics with the screening of simplified aromatic fragments.

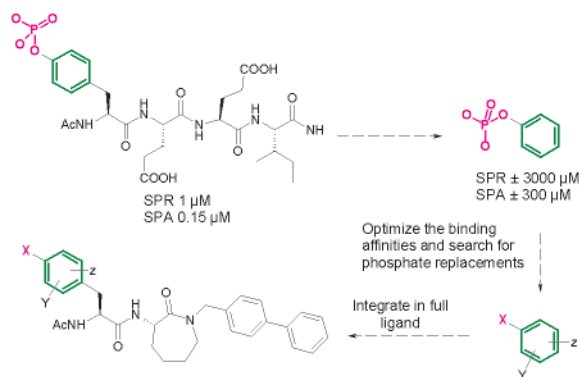
In addition to the discovery of original phosphate mimics, the aim of the study was the optimization of the aromatic ring substitution. These fragments would then eventually be incorporated into full inhibitors as phenyl phosphate replacements.

The second experimental observation followed the generation of Src SH2 crystals as cubes of 200  $\mu\text{m}$  width. This opened the way to a soaking strategy. The availability of large homogeneous batches of highly purified protein is an essential requirement to obtain reliable and reproducible crystallographic data. Here, taking advantage of high cell density fermentations and large-scale purifications, we have been able to produce single batches (even of 1.2 g) of highly concentrated Src SH2 protein, with no aggregation detectable (4–5 mg/mL, >99% pure as determined by SDS–PAGE and LC–ESI–MS analyses, not shown). In addition, these crystals displayed a molecule of citrate in the phosphotyrosine binding pocket. From the study of the crystal packing, we could see a channel of around 20  $\text{\AA}$  diameter that was large enough to let citrate diffuse from the crystal and be replaced by other fragments. In addition, it was observed that citrate was exchanged for a phosphate upon exposure of the crystals to a phosphate buffer solution.

**Table 1.** Src SH2 Binding Affinities of pYEEINH<sub>2</sub> and Phenyl Phosphate **2** Using SPR and SPA Assays

compound	Src SH2 IC <sub>50</sub> ( $\mu\text{M}$ )	
	SPR	SPA
pYEEINH <sub>2</sub>	1	0.15
H <sub>2</sub> O <sub>3</sub> PO <b>2</b>	$\pm 3000$	$\pm 300$

## Scheme 1

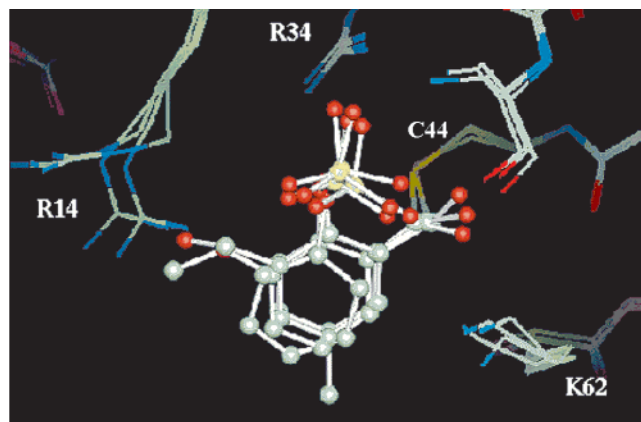


These crystals, when soaked with a solution of phenyl phosphate, gave rise to the expected exchange of ligands in the phosphotyrosine binding pocket. Study of the crystals revealed that the phenyl phosphate indeed did occupy the same position as the phenyl phosphate of the tetrapeptide pYEEI. Both phosphate groups interacted with arginines 14 and 34 (data not shown).

Thus our strategy was defined as follows. The potential utility of the small fragments replacing phenyl phosphate would be evaluated both in terms of *binding affinity* compared to that for phenyl phosphate and in terms of *positioning* compared to the phenyl phosphate of pYEEI peptide derived from the soaking experiments with Src SH2 crystals. Optimal fragments would then be incorporated into a full ligand as depicted in Scheme 1.

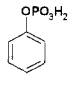
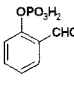
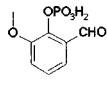
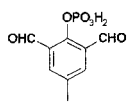
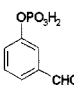
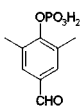
During the course of this program, a total of over 150 small ligands were evaluated for their binding affinity for Src SH2. The fragments that were evaluated either came from commercial sources or were synthesized on an individual basis or by using solid-phase or solution parallel synthesis.<sup>14,15</sup> All these fragments were soaked with crystals of Src SH2. About two-thirds of them did not dissolve the crystals, and measurements could be made. From these, around 20 gave rise to a structure in which the citrate molecule had been displaced by the fragment. Two distinct families of ligands were successfully soaked into the Src SH2 crystals: aromatic phosphates and polyacidic compounds. The former taught us about the ideal substitution of the aromatic ring, and the latter gave us insight about possible phosphate mimics. The present paper will describe some of the most significant data and the way the results were incorporated into the design of low nanomolar ligands of Src SH2.

**Optimization of the Aromatic Ring Substitution of Phosphotyrosine. Validation of the Strategy.** A series of about 120 aromatic phosphates, hydroxyphosphonates, and amidophosphonates were synthesized and studied for their binding affinity to Src SH2 in



**Figure 1.** Superimposition of **3**, **4**, **5**, and **2** in Src SH2.

comparison with phenyl phosphate itself. The summary of the data will be reported elsewhere.<sup>15</sup> In the aromatic phosphate series, no substituent in the 4-position of the aromatic ring relative to the phosphate group had a positive effect on the binding affinity except for a primary amine group. The same was true for the 2- and 3-positions. The only exception to this was seen on introduction of an aldehyde ortho to the phosphate (compounds **3–5**). Then a significant 4- to 10-fold

			
	<b>2</b>	<b>3</b>	<b>4</b>
SPR (IC <sub>50</sub> )	2–5 mM	0.3 mM	0.9 mM
SPA (IC <sub>50</sub> )	300 μM	80 μM	95 μM
			
	<b>5</b>	<b>6</b>	<b>7</b>
SPR (IC <sub>50</sub> )	0.5 mM	2.1 mM	5 mM
SPA (IC <sub>50</sub> )	39 μM	600 μM	nd*

\*Nd not determined

improvement of the binding affinity was obtained. This was specific to the ortho position to the phosphate as demonstrated by the fact that neither a meta nor a para aldehyde was able to display a similar enhancement (compounds **6** and **7**). A phosphate group was indispensable to the affinity because neither salicylaldehyde nor 2-hydroxy-3-formyl benzaldehyde displayed any binding affinity at all for Src SH2 (data not shown).

The presence of a unique solvent-accessible cysteine in the phosphotyrosine binding pocket of Src has been reported, and a few groups have tried to make use of it for gaining selectivity for Src vs other SH2 domains.<sup>16,17</sup> This interaction was indeed seen in the X-ray structures of the three phosphate aldehydes **3–5** with Src SH2 (Figure 1). When aldehydes **3–5** were compared with Src SH2, the phenyl ring and the aldehyde functions were perfectly superimposable. The three of them superimposed equally well with phenyl phosphate.

This encouraged us to incorporate an aldehyde function into our best Src SH2 ligand **1** to afford **8**. This resulted in a 40-fold improvement of the binding affinity

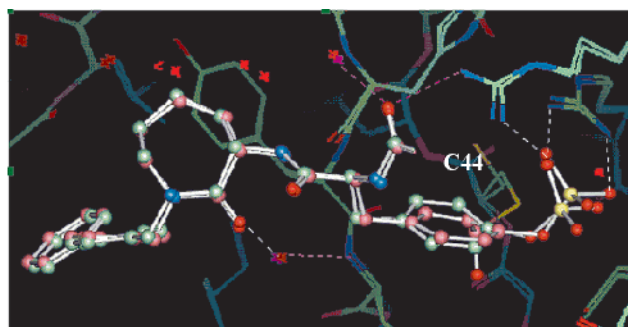
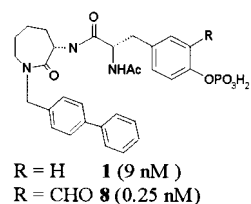


**Figure 2.** Superimposition of **1** (pink) and **8** (green) in Src SH2 crystals.

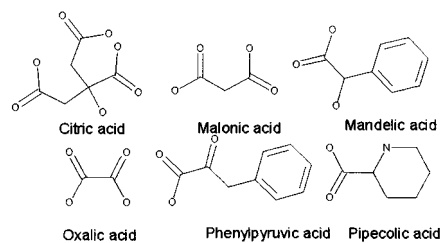
and selectivity for Src SH2 vs other SH2 domains<sup>18</sup> (i.e., Lck) using the SPA binding assay.



The costructures of **1** and **8** with Src SH2 displayed a perfect alignment of both ligands and the covalent hemithioacetal formed between cysteine 44 and the aldehyde function (Figure 2).

**Study of Phosphate Replacements.** Because the phosphate group can be cleaved by phosphatases, many authors have investigated nonhydrolyzable analogues. Earlier studies from Roques and then from Shoelson have demonstrated that phosphonates were good replacements that were stable to phosphatases.<sup>19</sup> The citrate in the phosphotyrosine binding pocket was a good starting point for the discovery of inhibitors devoid of the phosphate moiety.<sup>20</sup> Analysis of the crystal showed that the two carboxylic acid functions form an H-bond network similar to that for phosphate itself with arginines 14 and 34 and serine 36 of the binding pocket. In addition, H-bonds are formed between the citrate with lysine 62 and threonine 38.

From an ACD fragment database, a LUDI search in the phosphotyrosine binding pocket provided several fragments such as mandelic acid, malonic acid, pipercolic acid, oxalic acid, and phenylpyruvic acid. All incorpo-



rated one or two carboxylate functions.

None of these fragments showed any detectable binding affinity for Src SH2 within the range measured; neither did citrate itself. However, soaking was undertaken and proved to be successful for malonic and oxalic diacids. This provided an additional starting point for the finding of high-affinity non-phosphate ligands.



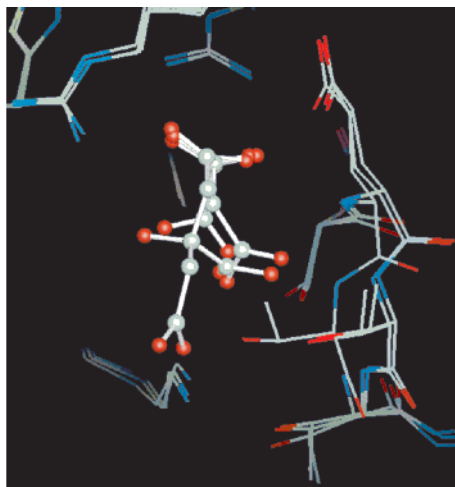
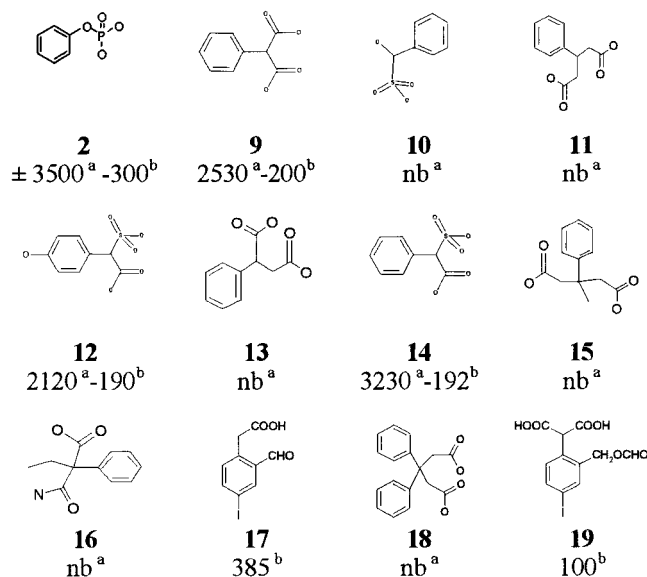


**Figure 3.** Superimposition of oxalic, malonic, and citric acids in Src SH2.

Oxalate and malonate in the SH2 domain of src make identical H-bonds, thereby forming an H-bond network similar to that found in the citrate structure. This indicated that the presence of this H-bond network is an essential recognition feature. In particular, the H-bond acceptors of citrate and malonate forming the H-bond network superimpose quite well (Figure 3). Compounds such as mandelic or pipercolic acid lack the H-bond acceptors that are required in order to complete the H-bond network, and hence, these compounds were not able to displace the citrate molecule in the binding pocket of Src SH2.

We undertook the evaluation of binding affinity and soaking of several aromatic compounds **9–19**, which incorporated acidic function(s). The glutaric acid ana-



logues **11**, **15**, **18** were inactive, along with phenyl succinic acid **13**. This pointed again to the fact that charge is not the only element controlling the recognition in this pocket. Derivatives **10** and **16** incorporating only one acidic function were inactive. However, **17** displayed about the same binding affinity as phenyl phosphate, suggesting that the interaction with the cysteine was probably able to compensate for the lack

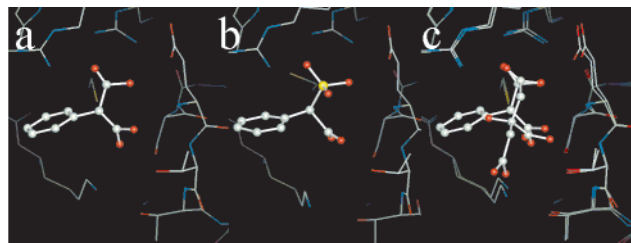
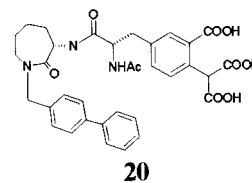


**Figure 4.** Soaking of phenylmalonic acid **9** (a) and 2-carboxybenzylsulfonic acid **12** (b) and superimposition of phenylmalonic acid **9** and citric acid (c) in Src SH2.

of a second charged interaction. In these experiments arylmalonate-type compounds such as **9**, **12**, **14**, and **19** behaved as very good substitutes for phenyl phosphate. This was once again confirmed by the fact that these compounds were able to displace the citrate molecule in the Src SH2 crystal. Parts a and b of Figure 4 show the structures of **9** and **12**, respectively, with Src SH2 confirming that a very similar H-bond network as in the citrate structure is present in the phosphotyrosine pocket. Indeed, the H-bond acceptors of the citrate and **9** superimpose extremely well (Figure 4c).

Several authors have reported on carboxylic acids as replacements for the phosphate moiety.<sup>21</sup> The early examples were in the shikimic acid pathway with the pioneering studies of Sikorski,<sup>21c</sup> while the bulk of the work was reported by T. Burke in the field of SH2 and phosphatase inhibitors.<sup>22</sup> However, at the time we undertook this work, no replacement had been found that was as active as the phosphate.<sup>23</sup> In addition, no structural information was available to show how these acids were interacting with the protein. Our data showed that the aromatic ring of phenyl malonate made essentially the same H-bond network as the phosphate of pYEEI, namely, the two conserved arginines 14 and 34, along with the H-bonds to serine 36. In addition, the aromatic ring was positioned in perfect alignment with the one in the peptide pYEEI (data not shown), suggesting that this moiety once incorporated into a full ligand would lead to high binding affinity for Src SH2.

To combine all the requirements for high binding affinity, we set ourselves the goal of synthesizing compound **20** with both the malonate moiety and a



carboxylic acid in the ortho position. The ortho carboxylate could either provide the third carboxylate from citric acid, as suggested by Figure 4c, or serve as precursor for an aldehyde or a formyloxymethylene in this position as in **17** or **19**, respectively. The chemistry of the synthesis of this compound did not turn out to be as straightforward as envisaged.<sup>24</sup>

Finally, a Heck<sup>25</sup> coupling reaction between methyl *N*-acetyldehydroglycinate and methyl 2-di-*tert*-butylmalonyl-5-iodobenzoate **22** obtained from 2,5-diiodobenzoic acid **21** gave dehydro-4-di-*tert*-butylmalonyl-3-carboxymethyl-*N*-acetylphenylalanine methyl ester **23**, which was coupled to the caprolactam derivative **24**<sup>9</sup>

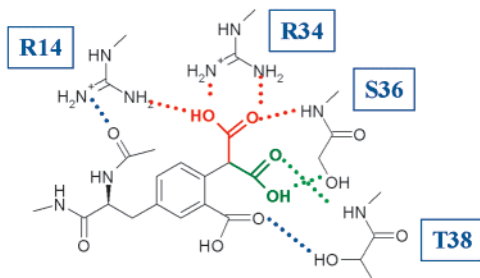
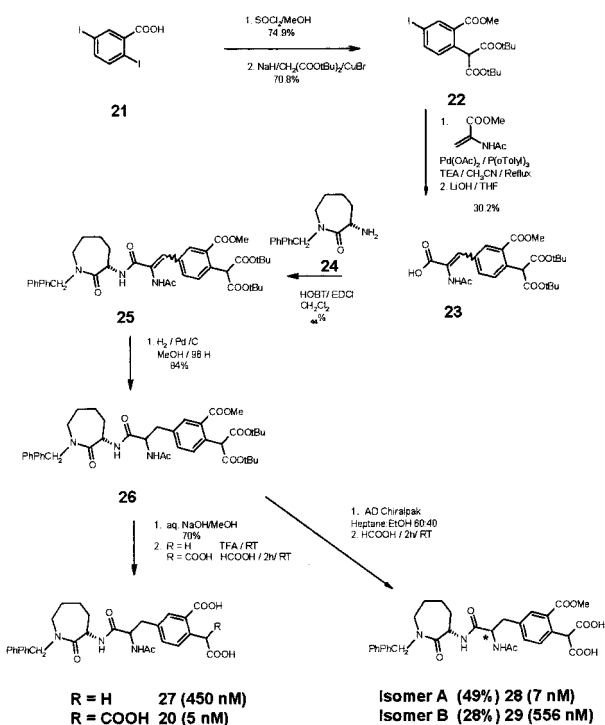


**Figure 5.** Schematic drawing of the two binding modes adopted by **27** with Src SH2. The carboxylic acid of **27** adopted the two orientations depicted in red and green, interacting with Arg34 and Ser36 or Ser36 and Thre38, respectively.

### Scheme 2



after saponification of the methyl ester to afford a good yield of the unsaturated derivative **25**, which could then be reduced by catalytic hydrogenation, and the methyl ester could be deprotected using basic hydrolysis to afford **26**. TFA deprotection of the *tert*-butyl esters gave the decarboxylated compound **27**. On the other hand, formic acid deprotection yielded the desired malonate **20** quantitatively (Scheme 2).

Interestingly, **27**, when soaked with the protein, demonstrated two modes of binding, strongly suggesting that the malonate analogue **20** would be much more tightly bound than the phenyl acetate (Figures 5 and 6). This indeed turned out to be the case, since the malonyl analogue **20** gave a 150-fold enhancement of the binding affinity when compared to the phenylacetate analogue **27**. Superimposition of the X-ray structures was excellent (data not shown). As for **27**, only one diastereoisomer of **20** having the *S*-stereochemistry (Figure 5) at the tyrosine mimic fragment was found in the protein. Separation of the diastereoisomeric mixture was undertaken at the stage of **26**. The two isomers were separated by chiral chromatography, and then each of them was hydrolyzed separately with formic acid to afford **28** and **29** in 49% and 28% yield, respectively

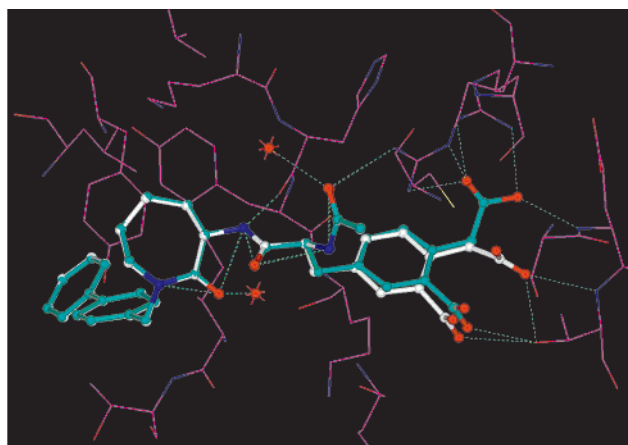


**Figure 6.** X-ray data of **27**. The two binding modes with Src SH2 are in green and white, respectively.

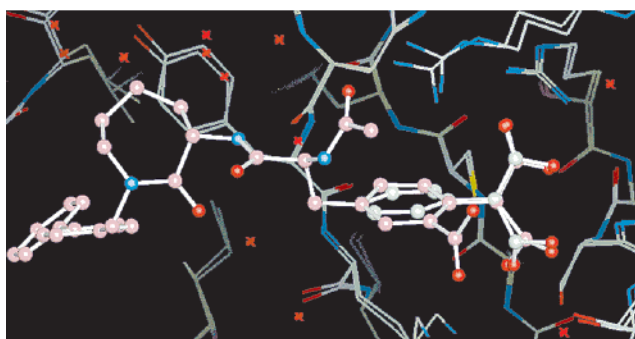


**Figure 7.** Superimposition of phenylmalonic acid **9** (green) with full-length inhibitor **20** (pink).

(Scheme 2). The two isomers demonstrated very different binding affinities for Src SH2 with  $\text{IC}_{50}$ 's of 7 and 556 nM, respectively. Gilmer<sup>11</sup> reported a 20-fold loss in Src SH2 affinity upon inversion of the chirality from L to D of the phosphotyrosine in the Ac-pYEEIE peptide. The above results suggest that isomer A has the natural configuration at the acetamido center.

The fact that the affinity of ester **28** was comparable to that of acid **20** is in line with the X-ray data of **20** showing that the ortho-acid function is only involved in one hydrogen bond interaction with Thre38. The superimposition of **20** with the initial phenyl malonate fragment **9** shows that the H-bond acceptors are located exactly in the same position in both structures. Aside from a slight tilt in the orientation of the phenyl ring, this resulted in identical interaction of the ligand with the protein (Figure 7). In addition, the superimposition of the X-ray structures of **1** and **20** (Figure 8) shows that the main part of both inhibitors superimpose very well, indicating that the replacement of the phenyl phosphate moiety in **1** has led to the same binding mode for both full-length inhibitors. However, it shows also that there are additional H-bond interactions in the phosphate binding site, leading to an increased affinity of **20** when compared to **1**.

### Conclusion

NMR screening was first described by Fesik as a powerful tool for drug discovery.<sup>26</sup> This method has been recently applied to the search for phosphotyrosine mimetics by the same group.<sup>27</sup> In this case, however, no fragment with the molecular size of phenyl phos-

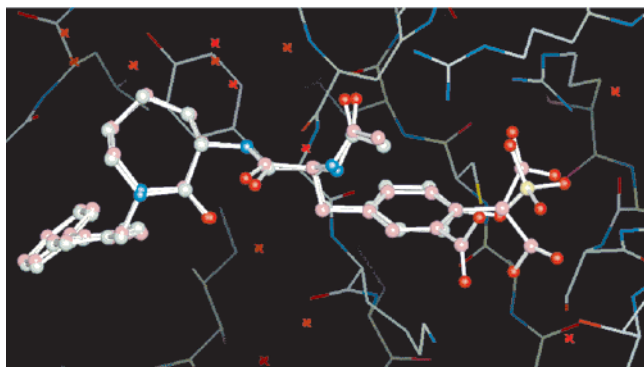


**Figure 8.** Superimposition of phosphate **1** (light green) and malonate **20** (pink).

phate demonstrated better binding affinity. More recently, X-ray screening has been demonstrated as a new alternative to complement existing screening methodologies.<sup>28</sup> In this work we report the use of crystal soaking for the purpose of rapid screening of small fragments with very low binding affinity for Src SH2. Structure determination of over 20 of these small aromatic compounds bound in the phosphotyrosine binding pocket allowed rapid selection of the best fragments to incorporate into full ligands. This new technology rapidly allowed us to identify low nanomolar range Src SH2 inhibitors devoid of phosphate groups. These compounds represent a step forward toward an Src SH2 inhibitor as a drug. Malonate-type inhibitors should not be hydrolyzed by phosphatases. In addition, **20** was shown to be stable over 24 h in rat and human plasma whereas **1** was much less stable ( $t_{1/2} = 0.6$  h in rat plasma) (data not shown). Finally, prodrug strategies are well-described for carboxylic acids, unlike for phosphates or phosphonates, and should allow cellular validation of the concept of SH2 domain inhibition.

## Experimental Section

**Production and Purification of Src SH2.** Plasmid pT7huSRC(145–251), containing the portion of the human Src gene coding for the SH2 domain (aa residues 145–251) under the control of the T7 promoter, was provided by ARIAD Pharmaceuticals (Cambridge, MA). *E. coli* BL21 (DE3) pT7huSRC(145–251) was grown in 6 L fermentors in high-cell-density conditions; protein expression was induced by addition of 1 mM IPTG at  $OD_{600nm} = 10–11$ , and cells were harvested after 8 h at 25 °C at  $OD_{600nm} = 44–45$ . The cell paste obtained (about 350 g, wet weight) was stored at –20 °C until use.

Protein purification was performed essentially by the method of Lynch et al.,<sup>29</sup> modified for large-scale purification. For a typical preparation, about 150 g of frozen cell paste were resuspended in two volumes of 50 mM potassium phosphate, pH 7.0, containing 250 mM NaCl, 2 mM EDTA, 5 mM DTT, and 1 mM PMSF under agitation at 4 °C for 30 min and then sonicated with a 25 mm probe in an ice bath by cycles of 1 min pulse + 1 min pause. After addition of two volumes of the same buffer, the lysate was centrifuged for 40 min at 30 000g. The supernatant was passed through a 0.22  $\mu$ m filter and was loaded on a 350 mL carboxysulfon (J. T. Baker) column, preequilibrated with 50 mM potassium phosphate, pH 7.0, containing 5 mM DTT. All chromatography steps were performed at a flow rate of 20 mL/min. After an extensive washing with equilibration buffer, the product was eluted from the column with a 40 min linear gradient from 0 to 1 M NaCl. Src-SH2, which eluted in the 0.5–0.8 M NaCl region (by SDS-PAGE analysis), was then concentrated by ultrafiltration with a 10 000 Da cutoff membrane, from 200 mL to a final volume

of 38–40 mL. After filtration at 0.22  $\mu$ m, the sample was loaded at 25 mL/min on a 6.4 L Sephacryl-100 HR (AmershamPharmacia, U.K.) column equilibrated with 20 mM potassium phosphate, pH 7.4, containing 0.5 M NaCl, 5 mM DTT, and 1 mM EDTA. Src-SH2 was found in the 0.65–0.70 CV region, where the protein was typically collected in a volume of 350–400 mL at a concentration of 4–5 mg/mL.

Protein identity and purity were routinely checked by SDS-PAGE, LC-ESI-MS, and N-terminal sequencing. Biochemical activity was tested by SPR (Biacore, Wallac), as described by E. Mandine et al. (manuscript in preparation).

**Preparation of Src SH2 Crystals.** From a 60–80 mg/mL solution of Src SH2 at 4 °C, the protein was placed in a 5  $\mu$ L dialysis button. The button was covered with a dialysis membrane (cutoff 3,500) and placed in a reservoir containing 1.5 mL of citrate buffer (pH 5.5)/DTT (10 mM). After 1 night, the dialysis button was placed in another reservoir containing milliQ H<sub>2</sub>O/DTT (10 mM). After 1 night, cubic-shaped monocrystals were observed (dimensions up to 300  $\mu$ m on a side). These crystals could then be conserved and handled in their liquor at room temperature.

**Soaking of the Crystals with Ligands.** The following solution was prepared: 15% PEG 400, 10% DMSO, MES buffer 100 mM, pH 5.5, 10 mM DTT. A total of 200  $\mu$ L of this solution was introduced in the well of a sitting drop crystallization container, and a total of 4.5  $\mu$ L of the same solution was placed on the bridge. Three or four Src SH2 crystals were introduced in a 4.5  $\mu$ L drop. The container was covered. After 2 h at room temperature, 0.5 or 2  $\mu$ L (as a function of the crystal's stability and/or of the ligand solubility) of a 100 mM ligand solution in 50% DMSO/Mes buffer 100 mM, pH 5.5, was added and the crystal was soaked overnight. If necessary, the pH was readjusted with diluted aqueous sodium hydroxide.

**Protein Crystallography.** Most data were collected at –170 °C on either a Mar345 imaging system or a MarCCD mounted on a rotating anode X-ray generator (GX21, Enraf Nonius). Some data were collected at the ESRF (BM14) or at LURE (W32). The data were processed using XDS<sup>30</sup> and refined using X-PLOR<sup>31</sup> based on a model provided by Ariad.<sup>32</sup> Model building and structure comparison were carried out using Quanta.<sup>33</sup> Prior to their comparison, all structures were superimposed using LSQKAB.<sup>34</sup> The resolution was in almost all cases below 2.1 Å. Merging of the data resulted in all cases in an  $R_{merge}$  better than 8.0%, and subsequent refinement resulted in  $R$  factors below 20%.

**Surface Plasmon Resonance Assay (SPR).** Real-time biomolecular interaction analysis was performed using a Biacore 2000 instrument (Biacore, Uppsala, Sweden) as described in ref 35. The fragments were assayed up to a concentration of 5 mM.

**Scintillation Proximity Assay (SPA).** Binding assays were conducted essentially as described in ref 10. The fragments were assayed up to a concentration of 1 mM.

**Chemistry. General Methods.** Analytical data were recorded for the compounds described using the following general procedures. Proton NMR spectra were recorded on a Bruker AC 300 MHz spectrometer, and chemical shifts were recorded in ppm ( $\delta$ ) from an internal tetramethylsilane standard in deuteriodimethyl sulfoxide unless otherwise specified below. Coupling constants ( $J$ ) were recorded in hertz. Mass spectra (MS) were recorded on an MS platform (micromass) and MS Autospec TOF (micromass) in electron impact, electrospray, and chemical ionization modes. Melting points (mp) were recorded on a Buchi 510 melting point apparatus and are uncorrected.

Flash chromatography was performed on silica gel 60H (Merck) using the solvent systems indicated below. For mixed-solvent systems, the volume ratios are given. Analytical HPLC was performed on a Merck HPLC system equipped with a Merck Hitachi L-4000A UV detector and reversed-phase C<sub>18</sub> column, kromasil 5  $\mu$ m at a flow rate of 1.5 mL min<sup>-1</sup>. All reactions were performed under a nitrogen atmosphere using magnetic stirring. Reactions were monitored by thin-layer chromatography (TLC) on precoated plates of silica gel 60F<sub>254</sub>



(layer thickness, 0.25 mm; E. Merck, Darmstadt). Anhydrous magnesium sulfate (MgSO<sub>4</sub>) was used routinely to dry the combined organic layers from extractions. Solvent was routinely removed in vacuo using a rotary evaporator followed by evacuation with a vacuum pump.

Commonly used abbreviations are EtOAc (ethyl acetate), MeOH (methanol), DMF (*N,N*-dimethylformamide), THF (tetrahydrofuran), and CH<sub>2</sub>Cl<sub>2</sub> (dichloromethane).

**Synthesis of Small Fragments and Full Ligands.** All aromatic phosphates were synthesized according to Deprez et al.<sup>14,15</sup> Phenyl malonic acid **9**, 3-phenylglutaric acid **17**, 4-hydroxysulfonylphenylacetic acid **12**, and phenylsuccinic acid **13** were purchased from Aldrich. Hydroxytoluenesulfonic acid **10**, 2-carbamoylphenyl butyric acid **18**, sulfonylphenylacetic acid benzoate[4-iodo-2-(methoxycarbonyl)phenyl]propanedioic acid, 1,3-bis(1,1-dimethylethyl) ester **22** and 3-methyl-3-phenylglutaric acid **15** were purchased from Salor. 3-Diphenylglutaric acid **18** was synthesized as described in the literature.<sup>36</sup> Methyl 2-acetamidoacrylate was purchased from Aldrich.

**Methyl 2-Di-*tert*-Butylmalonate-5-iodobenzoate[4-iodo-2-(methoxycarbonyl)phenyl]propanedioic Acid, 1,3-Bis(1,1-dimethylethyl) Ester **22**.** A total of 40 g (107 mmol) of 2,5-diiodobenzoic acid **21** was dissolved in 960 mL of methanol, the flask was cooled in an ice bath, and 27.2 mL (375 mmol) of thionyl chloride were added dropwise. The solution was refluxed for 23 h, then concentrated, poured onto water, and extracted with EtOAc. The organic extracts were washed with a saturated aqueous solution of NaHCO<sub>3</sub> and then with brine, and the organic extracts were dried and concentrated to afford 41.05 g of the expected ester as a cream-colored solid. Recrystallization from hot diisopropyl ether gave 31.08 g (74.9%) of methyl 2,5-diiodobenzoate as cream-colored crystals. Mp 79 °C; NMR (CDCl<sub>3</sub>) δ 3.94 (s, 3H), 7.45 (dd, 1H), 7.69 (d, 1H), 8.11 (d, 1H).

A 1 L flask was equipped with a thermometer, an addition funnel, and a reflux condenser. A total of 7.43 g NaH (50% oil suspension, 154.8 mmol) was introduced followed by 180 mL of dioxan. A total of 34.8 mL (155.04 mmol) of di-*tert*-butyl malonate dissolved in 240 mL of dioxan was added dropwise to the previous solution maintained between 20 and 25 °C. The mixture was stirred at room temperature for 30 min after the addition until the evolution of hydrogen had stopped. Then a total of 22.16 g (154.5 mmol) of CuBr was added, and the dark-green suspension was stirred for 15 min at room temperature. An amount of 30 g (77.32 mmol) of methyl 2,5-diiodobenzoate **21** in 360 mL of dioxan was added. The resulting mixture was refluxed for 16 h, then cooled to room temperature, poured in a saturated aqueous solution of NH<sub>4</sub>Cl, and extracted with EtOAc. The organic extracts were washed with brine, dried, and evaporated to afford 51.4 g of crude product. Flash chromatography (1.4 kg of silica, CH<sub>2</sub>-Cl<sub>2</sub>) gave expected methyl 2-di-*tert*-butylmalonate-5-iodobenzoate[4-iodo-2-(methoxycarbonyl)phenyl]propanedioic acid, 1,3-bis(1,1-dimethylethyl) ester **22** as a colorless oil (26.08 g, 70.8%). *R*<sub>f</sub> = 0.3 (RP-18F<sub>254</sub>Merck, MeOH/H<sub>2</sub>O, 85/15); NMR (CDCl<sub>3</sub>) δ 1.48 (s, 9H), 3.88 (s, 3H), 5.43 (s, 1H), 7.28 (d, 1H), 7.84 (dl, 1H), 8.30 (d, 1H); MS *m/z* 475 (M - H)<sup>-</sup>, 499 (M + Na)<sup>+</sup>.

**Dehydro-4-di-*tert*-butylmalonyl-3-carboxymethyl-*N*-acetylphenylalanine[4-[2-(acetylamino)-2-carboxyethenyl]-2-(methoxycarbonyl)phenyl]propanedioic Acid, 1,3-Bis(1,1-dimethylethyl) Ester **23**.** An amount of 26.08 g (54.75 mmol) of [4-iodo-2-(methoxycarbonyl)phenyl]propanedioic acid, 1,3-bis(1,1-dimethylethyl) ester **22** was introduced into a 2 L flask and dissolved in 1 L of CH<sub>3</sub>CN. An amount of 15.7 g (109.5 mmol) of methyl 2-acetamidoacrylate was added to the mixture followed by 9.6 mL (68.93 mmol) of triethylamine, 711.6 mg (3.17 mmol) of Pd (OAc)<sub>2</sub>, and 1.67 g (5.48 mmol) of tri-*o*-tolylphosphine. The suspension was refluxed for 30 h, then brought to room temperature and evaporated to about one-third of its volume. The suspension was poured into a saturated aqueous solution of NaHCO<sub>3</sub> and extracted with EtOAc. The organic extracts were washed with brine, dried, and evaporated to dryness to afford 37.88 g of crude product

as a black oil. Flash chromatography (1.4 kg silica, CH<sub>2</sub>Cl<sub>2</sub>/MeOH, 97.5:2.5) gave 8.14 g (30.2%) of the expected material as a cream-colored foam. *R*<sub>f</sub> = 0.12 (SiO<sub>2</sub>F<sub>254</sub>Merck) CH<sub>2</sub>Cl<sub>2</sub>/EtOAc, 90/10; NMR mixture *Z/E* 50/50 δ 1.49 (s, 18H), 2.17 (ls, 1H), 3.87 (s, 3H), 3.89 (s, 3H), 5.48 (s, 1H), 7.01 (ls, 1H), 7.31 (ls, 1H), 7.49 (d, 1H), 7.58 (ld, 1H), 8.12 (ls, 1H); MS *m/z* 490 (M - H)<sup>-</sup>, 390 (MH - OtBu), 316 (390 - OtBu).

A total of 4.14 g of the previous compound (8.42 mmol) was dissolved in 170 mL of THF and treated with a solution of 371.1 mg (8.84 mmol) of LiOH·H<sub>2</sub>O in 57 mL of H<sub>2</sub>O. The resulting yellow solution was stirred for 1.5 h at room temperature and then poured into 400 mL of H<sub>2</sub>O and 11.5 mL of 1 M HCl and extracted with EtOAc. The organic extracts were washed with brine, dried, and concentrated under vacuum to afford 4.17 g of the expected [4-[2-(acetylamino)-2-carboxyethenyl]-2-(methoxycarbonyl)phenyl]propanedioic acid, 1,3-bis(1,1-dimethylethyl) ester **23** as a cream-colored foam. *R*<sub>f</sub> = 0.23 (RP-18F<sub>254</sub>Merck, MeOH/H<sub>2</sub>O, 85/15); NMR δ 1.43 (s, 1H), 1.99 (sl, 1H), 3.8 (s, 1H), 5.26 (s, 1H), 7.16 (sl, 1H), 7.64 (dd, 1H), 7.70 (d, 1H), 7.98 (sl, 1H), 9.28 (sl, 1H); MS *m/z* 476 (M - H)<sup>-</sup>, 432 (M - H - CO<sub>2</sub>), 390, 289, 232.

**[4-[2-(Acetylamino)-3-[[3-*S*]-1-[[1,1'-biphenyl]-4-yl]methyl]-2-oxohexahydro-1*H*-azepin-3-yl]amino]-3-oxo-1-propenyl]-2-(methoxycarbonyl)phenyl]propanedioic Acid, 1,3-Bis(1,1-dimethylethyl) Ester **25**.** An amount of 3.55 g (7.43 mmol) of [4-iodo-2-(methoxycarbonyl)phenyl]propanedioic acid, 1,3-bis(1,1-dimethylethyl) ester **22** was dissolved in 105 mL of CH<sub>2</sub>Cl<sub>2</sub> and 35 mL of DMF in a 500 mL flask under argon and cooled in an ice bath. An amount of 1.42 g (7.43 mmol) of 1-(3-dimethylaminopropyl)-3-ethylcarbodiimide hydrochloride (EDCI) was added followed by 1 g (7.43 mmol) of 1-hydroxybenzotriazole (HOBT). The solution was stirred for 30 min at room temperature and then added dropwise to a cooled solution of 2.19 g (7.43 mmol) of amine (3*S*)-amino-1-[[1,1'-biphenyl]-4-yl]methyl]hexahydro-2*H*-azepin-2-one **24**<sup>9</sup> in 70 mL of dichloromethane (0 °C). The resulting solution was stirred for 16 h at room temperature, then poured into H<sub>2</sub>O, and extracted with EtOAc. The organic extracts were washed with an aqueous solution of NaHCO<sub>3</sub> and then brine, dried, and concentrated to afford 5.09 g of crude product. Flash chromatography (1 kg of silica, CH<sub>2</sub>-Cl<sub>2</sub>/MeOH, 97.5:2.5) gave 2.47 g of the expected compound as a colorless oil (44.15%). *R*<sub>f</sub> = 0.23 (RP-18F<sub>254</sub>Merck, MeOH/H<sub>2</sub>O, 85/15); HPLC CH<sub>3</sub>CN/H<sub>2</sub>O, 75/25, 0.01% TFA, 1.5 mL/min, 96 bar, 230 nm, 7.38 min, 91%; NMR δ 1.08–2 (m, 6H), 1.44 (s, 9H), 2.06 (s, 3H), 3.30 (m, 2H), 3.65 (dd, 2H), 3.82 (s, 3H), 4.7 (m, 1H), 5.29 (s, 1H), 7.20 (s, 1H), 7.36 (m, 4H), 7.46 (m, 2H), 7.65 (m, 4H), 7.8 (dd, 1H), 8.11 (d, 1H), 9.71 (s, 1H).

**[4-[2-(Acetylamino)-3-[[3-*S*]-1-[[1,1'-biphenyl]-4-yl]methyl]-2-oxohexahydro-1*H*-azepin-3-yl]amino]-3-oxo-1-propenyl]-2-(methoxycarbonyl)phenyl]propanedioic Acid, 1,3-Bis(1,1-dimethylethyl) Ester **26**.** A hydrogenating flask was charged with 2.47 g (3.28 mmol) of [4-[2-(acetylamino)-3-[[3-*S*]-1-[[1,1'-biphenyl]-4-yl]methyl]-2-oxohexahydro-1*H*-azepin-3-yl]amino]-3-oxo-1-propenyl]-2-(methoxycarbonyl)phenyl]propanedioic acid, 1,3-bis(1,1-dimethylethyl) ester **25** dissolved in 282 mL of methanol, and 815 mg of 10% palladium on carbon (E10ND charge 7389) was added. The mixture was placed under 1760 mbar of hydrogen for 96 h, and then the suspension was filtered over Celite and concentrated to afford 2.32 g of crude material purified by flash chromatography (300 g of silica, CH<sub>2</sub>Cl<sub>2</sub>/MeOH, 97.5:2.5) to give 1.86 g (74.5%) of the pure, reduced compound as a white foam. HPLC (CH<sub>3</sub>CN/H<sub>2</sub>O, 75:25, 0.01% TFA, 1.5 mL/min, 96 bar, 230 nm, 7.76 min, 52.4%, 7.96 min, 43.2%; NMR 6:4 mixture of diastereoisomers δ 1.18–1.85 (m, 6H), 1.42 (s, 18H), 1.77 (s, 3H), 2.75 and 2.82 (2d, 1H), 3.03 and 3.14 (2dd, 1H), 3.25 and 3.58 (2m, 2H), 3.80 (ls, 3H), 4.31–4.76 (m, 3H), 5.23 (ls, 1H), 7.24 (d), 7.36, 7.44, 7.46 (t), 7.64, 7.86 (12H), 8.14, 8.15, 8.21 (3d, 2H); MS *m/z* 778 (M + Na)<sup>+</sup>, 754 (M - H)<sup>-</sup>, 700 (MH<sup>+</sup> - t-Bu)<sup>+</sup>, 695 (M - H - NHAc)<sup>-</sup>, 644 (700<sup>+</sup> - tBu)<sup>+</sup>, 167 (PhPhCH<sub>2</sub><sup>+</sup>).

A total of 1.5 g (1.98 mmol) of the previous compound was dissolved in 89 mL of THF and treated with 9 mL of aqueous

1 M NaOH (4 mmol). The mixture was heated to 50 °C for 7.5 h and then poured into water and acidified with 13.25 mL (13.25 mmol) of 1 N HCl. The mixture was extracted with EtOAc, and the organic extracts were washed with brine, dried, concentrated (1.47 g of crude), and purified by flash chromatography (185 g of silica, CH<sub>2</sub>Cl<sub>2</sub>/MeOH, 96.5:3.5) to give the first fraction of 285 mg (19%) of the recovered starting material as a white foam. Then the product was eluted from the column with CH<sub>2</sub>Cl<sub>2</sub>/MeOH/AcOH, 96.5:3.5:1.5 to give 897.8 mg (61%) of the expected material as a white foam. *R<sub>f</sub>* = 0.29 (RP-18F<sub>254</sub>Merck, MeOH/H<sub>2</sub>O, 85/15); HPLC (CH<sub>3</sub>CN/H<sub>2</sub>O, 75:25, 0.01% TFA, 1.5 mL/min, 96 bar, 230 nm, 4.57 min, 92.2%; NMR 6:4 mixture of diastereoisomers δ 1.16 and 1.66 (2m, 2H), 1.39, 1.62–1.87 (m, 4H), 1.41 (s, 18H), 1.77 (s, 3H), 2.74 and 2.81 (2ld, 1H), 3.03 and 3.14 (2dd, 1H), 3.27 and 3.58 (2m, 2H), 4.31–4.76 (m, 3H), 5.43 (ls, 1H), 7.23 (m), 7.36, 7.47, 7.64, 7.88 (12H), 8.13, 8.19, 8.22 (3d, 2H), 13.04 (sl, 1H); MS *m/z* 740 (M – H)<sup>–</sup>, 666 (740, O – t-Bu)<sup>–</sup>.

**[4-[2-(Acetylamino)-3-[[[(3S)-1-[[1,1'-biphenyl]-4-yl]methyl]-2-oxohexahydro-1H-azepin-3-yl]amino]-3-oxo-1-propenyl]-2-carboxyphenyl]propanedioic Acid 20 and 4-[2-(Acetylamino)-3-[[[(3S)-1-[[1,1'-biphenyl]-4-yl]methyl]-2-oxohexahydro-1H-azepin-3-yl]amino]-3-oxo-1-propenyl]-2-carboxybenzenoic Acid 27.** A total of 8.6 mg of [4-[2-(acetylamino)-3-[[[(3S)-1-[[1,1'-biphenyl]-4-yl]methyl]-2-oxo-hexahydro-1H-azepin-3-yl]amino]-3-oxo-1-propenyl]-2-carboxyphenyl]propanedioic acid, 1,3-bis(1,1-dimethylethyl) ester **26** (0.119 mmol) was dissolved in 2.2 mL of 98% HCOOH (58.31 mmol). The solution was stirred for 2 h at room temperature and then partitioned between water and EtOAc. The organic extracts were washed with water and brine, dried, and concentrated to afford 68.1 mg of crude material as a white foam. This material was triturated with cold diethyl ether and filtered to afford 64 mg (85.6%) of the expected material [4-[2-(acetylamino)-3-[[[(3S)-1-[[1,1'-biphenyl]-4-yl]methyl]-2-oxohexahydro-1H-azepin-3-yl]amino]-3-oxo-1-propenyl]-2-carboxyphenyl]propanedioic acid **20** as a white powder. *R<sub>f</sub>* = 0.12 (SiO<sub>2</sub>F<sub>254</sub>Merck60, CH<sub>2</sub>Cl<sub>2</sub>/MeOH/AcOH, 80/20/5); HPLC, CH<sub>3</sub>CN/H<sub>2</sub>O, 65/35, 0.01% TFA, 1 mL/min, 77 bar, 230 nm, 2.82 min, 90%; NMR 1:1 mixture of diastereoisomers δ 1.12–1.89 (m, 6H), 1.78 (s, 3H), 2.77 (dd, 1H), 3.26–3.58 (m, 2H), 3.68 (dd, 1H), 4.31–4.77 (m, 3H), 5.41 (sl, 1H), 7.23 (dd), 7.36, 7.46, 7.66, 7.85 (12H), 8.17, 8.23 (sl, 2H); MS *m/z* 650 (MNa<sup>+</sup> – 2H)<sup>–</sup>, 628 (M – H)<sup>–</sup>; HRMS calcd 630.2451, found 630.2454.

A total of 17 mg (0.027 mmol) of [4-[2-(acetylamino)-3-[[[(3S)-1-[[1,1'-biphenyl]-4-yl]methyl]-2-oxohexahydro-1H-azepin-3-yl]amino]-3-oxo-1-propenyl]-2-carboxyphenyl]propanedioic acid **20** was dissolved in 4 mL of methanol and warmed for 3 h at 50–60 °C. The solution was filtered, concentrated, and recrystallized in 20 mL of diethyl ether to afford 15.7 mg (99%) of the expected compound 4-[2-(acetylamino)-3-[[[(3S)-1-[[1,1'-biphenyl]-4-yl]methyl]-2-oxohexahydro-1H-azepin-3-yl]amino]-3-oxo-1-propenyl]-2-carboxybenzenoic acid **27** as a white powder. *R<sub>f</sub>* = 0.43 (SiO<sub>2</sub>F<sub>254</sub>Merck60, CH<sub>2</sub>Cl<sub>2</sub>/MeOH/AcOH, 80/20/5); HPLC CH<sub>3</sub>CN/H<sub>2</sub>O, 65/35, 0.01% TFA, 1 mL/min, 77 bar, 230 nm, 3.2 min, 86%; NMR 6:4 mixture of diastereoisomers δ 1.12–1.90 (m, 6H), 1.77 (s, 3H), 2.76 (dd, 1H), 3.02, 3.12 (dd, 1H), 3.26–3.58 (m, 2H), 3.84 (s, 2H), 4.31–4.78 (m, 4H), 7.19, 7.35, 7.36, 7.46, 7.63, 7.66, 7.81 (12H), 8.08 (sl, 1H), 8.29 (sl, 1H), 12.56 (sl, 2H); MS *m/z* 584<sup>–</sup> (M – H), 540<sup>–</sup> (M – H – CO<sub>2</sub>); HRMS calcd 586.2553, found 586.2584.

**[4-[2-(Acetylamino)-3-[[[(3S)-1-[[1,1'-biphenyl]-4-yl]methyl]-2-oxohexahydro-1H-azepin-3-yl]amino]-3-oxo-1-propenyl]-2-(methoxycarbonyl)phenyl]propanedioic Acids 28 (Iso A) and 29 (Iso B).** The 2 diastereoisomers of **26** were separated by chiral HPLC before ester hydrolysis. The following were used for the AD chiralpack column: heptane/ethanol, 60/40, 1.5 mL/min, 210 nm, 6.89 min (iso A), 10.92 min (iso B). From 145 mg of **26**, 87 mg (0.115 mmol) of iso A and 55 mg (0.072 mmol) of iso B were obtained. Each of them was hydrolyzed separately using 3.6 mL (95.4 mmol) and 2.26 mL (59.90 mmol) of 98–100% formic acid respectively in 2 and 0.4 mL of CH<sub>2</sub>Cl<sub>2</sub>, respectively. The suspensions were for stirred 2 h at 20 °C and then poured into water and extracted

with EtOAc. The organic extracts were washed with brine, dried, and concentrated. The residues were crystallized in Et<sub>2</sub>O to give 59.7 mg (80.6%) and 29.6 mg (63.2%) of pure **28** (iso A) and **29** (iso B), respectively. **28**: HPLC, CH<sub>3</sub>CN/H<sub>2</sub>O, 75:25, 0.01% TFA, 1 mL/min, 60 bar, 230 nm, 3.14 min, 97.64%; NMR δ 1.20–1.96 (m, 6H), 1.94 (s, 3H), 3.00 and 3.24 (dd, 2H), 3.32 and 3.58 (dd, 2H), 3.84 (s, 3H), 4.58 and 4.72 (m, 2H), 4.68 (m, 1H), 4.73 (m, 1H), 5.42 (s, 1H), 7.20–7.63 (m, 12H), 7.93 (m, 1H), 8.39 (m, 1H). **29**: HPLC, CH<sub>3</sub>CN/H<sub>2</sub>O, 75:25, 0.01% TFA, 1 mL/min, 59 bar, 230 nm, 2.88 min, 94.7%; NMR δ 1.23–1.96 (m, 6H), 3.04 and 3.17 (dd, 2H), 3.3 and 3.57 (m, 2H), 3.85 (s, 3H), 4.54 and 4.73 (m, 2H), 4.64 (m, 1H), 4.72 (m, 1H), 5.37 (s, 1H), 7.34 (m, 3H), 7.42 (m, 3H), 7.50 (dd, 1H), 7.59 (m, 4H), 7.91 (d, 1H).

**Acknowledgment.** This work was done during the course of collaboration with ARIAD Pharmaceuticals. We are grateful to Tom Sawyer, M. Weigele, R. Bohacek, and the entire group of scientists there for stimulating discussions and interactions. We thank M. R. Van Schravendyck for providing the clones and procedures for Src SH2 production and purification.

## References

- Brown, M. T.; Cooper, J. A. Regulation, Substrates and Functions of Src. *Biochim. Biophys. Acta* **1996**, *1287*, 121–149.
- Soriano, P.; Montgomery, C.; Geske, R.; Bradley, A. Targeted disruption of the c-src proto-oncogene leads to osteopetrosis in mice. *Cell* **1991**, *64* (4), 693–702.
- Boyce, B. F.; Yoneda, T.; Lowe, C.; Soriano, P.; Mundy, G. R. Requirement of pp60c-src expression for osteoclasts to form ruffled borders and resorb bone in mice. *J. Clin. Invest.* **1992**, *90* (4), 1622–1627.
- For a general review on SH2 domains, see: Sawyer, T. K. Src Homology-2 Domains: Structure, Mechanisms and Drug Discovery *Biopolymers* **1998**, *47*, 243–261.
- For a general review on SH3 domains, see: Dalgarno, D. C.; Bottfield, M. C.; Rickles, R. J. SH3 Domains and Drug Design: Ligands, Structure and Biological Functions. *Biopolymers* **1998**, *43* (5), 383–400.
- Schwartzberg, P. L.; Xing, L.; Hoffmann, O.; Lowell, C. A.; Garrett, L.; Boyce, B. F.; Varmus, H. E. R. Rescue of osteoclast function by transgenic expression of kinase-deficient Src in src-/- mutant mice. *Genes Dev.* **1997**, *21*, 2835–2844.
- Songyang, Z.; Shoelson, S. E.; Chaudhuri, M.; Gish, G.; Pawson, T.; Haser, W. G.; King, F.; Roberts, T.; Ratnofsky, S.; Lechleider, R. J.; Neel, B. J.; Birge, R. B.; Fajardo, G. E.; Chou, M. M.; Hanafusa, H.; Schaffhausen, B.; Cantley, L. C. SH2 domains recognize specific phosphopeptide sequences. *Cell* **1993**, *72*, 767–778.
- Alonso, G.; Koegl, M.; Mazurenko, M.; Courtneidge, S. A. Sequence requirements for binding of Src family tyrosine kinases to activated growth factor receptors. *J. Biol. Chem.* **1995**, *270*, 9840–9848.
- Deprez, P.; Baholet, I.; Bulet, S.; Lange, G.; Schoot, B.; Vermond, A.; Mandine, E.; Lesuisse, D. Discovery of highly potent Src SH2 binders: Structure–activity studies and X-ray structures. *Bioorg. Med. Chem. Lett.* In press.
- (a) Mandine, E.; Gofflo, D.; Jean-Baptiste, V.; Gaillard-Kelly, M.; Zoller, M.; Baron, R.; Lesuisse, D. The reactivation of Csk-inactivated Src by phosphopeptides is correlated to their ability for the SH2 domain. *J. Bone Miner. Res.* **1998**, *23*, S221. (b) Mandine, E.; Gofflo, D.; Jean-Baptiste, V.; Sarubbi, E.; Touyer, G.; Deprez, P.; Lesuisse, D. Src homology-2 domain binding assays by scintillation proximity and surface plasmon resonance. *J. Mol. Recognit.* **2001**, *14*, 254–260.
- Gilmer, T.; Rodriguez, M.; Jordan, S.; Crossby, R.; Alligood, K.; Green, M.; Kimery, M.; Wagner, C.; Kinder, D.; Charifson, P.; Hassel, A. M.; Willard, D.; Luther, M.; Rusnak, D.; Sternbach, D. D.; Mehrotra, M.; Peel, M.; Shampine, L.; Davis, R.; Robbins, J.; Patel, I. R.; Kassel, D.; Burkhart, W.; Moyer, M.; Bradshaw, T.; Berman, J. Peptide inhibitors of Src SH3SH2 phosphoprotein interactions. *J. Biol. Chem.* **1994**, *269* (50), 31711–31719.
- Sibley, C. P.; Bauman, K. F.; Firth, J. A. Molecular charge as a determinant of macromolecule permeability across the fetal capillary endothelium of the guinea-pig placenta. *Cell Tissue Res.* **1983**, *229* (2), 365–377. Aubert, L.; Motais, R. Molecular features of organic anion permeability in ox red blood cell. *J. Physiol.* **1975**, *246* (1), 159–179. Allentoff, A. J.; Mandiyan, S.; Liang, H.; Yuryev, A.; Vlattas, I.; Duelfer, T.; Sytwu, I.-I.; Wennogle, L. P. Understanding the cellular uptake of phosphopeptides. *Cell Biochem. Biophys.* **1999**, *31* (2), 129–140.



- (13) Malmqvist, M. Biospecific interaction analysis using biosensor technology. *Nature* **1993**, *361*, 186–187.
- (14) Deprez, P.; Lesuisse, D. Convenient phosphorylation of alcohols with a supported phosphite: synthesis of free phosphates and phosphate esters. *Tetrahedron Lett.*, in press.
- (15) Deprez, P.; Mandine, E.; Gofflo, D.; Meunier, S.; Lesuisse, D. Small ligands interacting with the phosphotyrosine binding pocket of the Src SH2 protein. *Bioorg. Med. Chem. Lett.*, in press.
- (16) Violette, S. M.; Shakespeare, W. C.; Bartlett, C.; Guan, W.; Smith, J. A.; Rickles, R. J.; Bohacek, R. S.; Holt, D. A.; Baron, R.; Sawyer, T. K. A Src SH2 selective binding compound inhibits osteoclast-mediated resorption. *Chem. Biol.* **2000**, *7* (3), 225–235. Aligood, K. J.; Charifson, P. S.; Crosby, R.; Consler, T. G.; Feldman, P. L.; Gampe, R. T.; Gilmer, T. M.; Jordan, S. R.; Milstead, M. W.; Mohr, C.; Peel, M. R.; Rocque, W.; Rodriguez, M.; Rusnak, D. W.; Shewchuk, M. L.; Sternbach, D. D. The formation of a covalent complex between a dipeptide ligand and the SRC SH2 domain. *Bioorg. Med. Chem. Lett.* **1998**, *8*, 1189–1194. Shakespeare, W. C.; Bohacek, R. S.; Narula, S. S.; Azimioara, M. D.; Yuan, R. W.; Dalgarno, D. C.; Madden, L.; Botfield, M. C.; Holt, D. A. An efficient synthesis of a 4'-phosphonodifluoromethyl-3'-formyl-phenylalanine containing Src SH2 ligand. *Bioorg. Med. Chem. Lett.* **1999**, *9* (21), 3109–3112.
- (17) Charifson, P. S.; Shewchuk, L. M.; Rocque, W.; Hummel, C. W.; Jordan, S. R.; Mohr, C.; Pacofsky, G. J.; Peel, M. R.; Rodriguez, M.; Sternbach, D. D.; Consler, T. G. Peptide Ligands of pp60<sup>src</sup> SH2 Domains: A Thermodynamic and Structural Study. *Biochemistry* **1997**, *36*, 6283.
- (18) This binding affinity improvement was higher than anticipated compared with the affinities of the small fragments. In the literature, the binding affinity improvements observed by incorporating an aldehyde function on the phosphotyrosine of ligands have turned out to be smaller than predicted on the basis of the formation of a covalent bond. One possible reason advanced by Charifson et al.<sup>17</sup> has been the dramatic decrease of entropy observed upon ITC studies and the loss of rotational and translational degrees of freedom of the phosphotyrosine ring. In fact, we have conducted such studies as well (D. Lafitte et al., to be published elsewhere), and the  $\Delta\Delta S$  between 36 and 2 of  $39.2 \text{ J K}^{-1} \text{ mol}^{-1}$  confirmed these observations, while the  $\Delta\Delta H$  of  $10.8 \text{ kJ/mol}$  could be accounted for by covalent bond formation.
- (19) Marseigne, I.; Roques, B. P. Synthesis of New Amino Acids Mimicking Sulfated and Phosphorylated Tyrosine Residues. *J. Org. Chem.* **1988**, *53*, 3621–3624. Domchek, S. M.; Auger, K. R.; Chatterjee, S.; Burke, T. R.; Shoelson, S. E. Inhibition of SH2 domain/phosphoprotein association by a nonhydrolyzable phosphonopeptide. *Biochemistry* **1992**, *31*, 9865–9870. Burke, T. R.; Smyth, M. S.; Otaka, A.; Nomizu, M.; Roller, P. R.; Wolf, G.; Case, R.; Shoelson, S. E. Nonhydrolyzable phosphotyrosyl mimetics for the preparation of phosphatase resistant SH2 domain inhibitors. *Biochemistry* **1994**, *33*, 6490–6494.
- (20) Shakespeare, W.; Yang, M.; Bohacek, R.; Cerasoli, F.; Stebbins, K.; Sundaramoorthi, R.; Azimiora, M.; Vu, C.; Pradeepan, S.; Metcalf, C.; Haraldson, C.; Merry, T.; Dalgarno, D.; Narula, S.; Hatada, M.; Lu, X.; Van Schravendijk, M. R.; Adams, S.; Violette, S.; Smith, J.; Guan, W.; Bartlett, C.; Herson, J.; Iulucci, J.; Weigle, M.; Sawyer, T. Structure-based design of an osteoclast-selective, nonpeptide src homology 2 inhibitor with in vivo antiresorptive activity. *PNAS* **2000**, *97*, 9373–9378.
- (21) (a) Phosphate mimics for this system have been reviewed recently: Burke, T. R., Jr.; Gao, Y.; Yao, Z.-J. Phosphotyrosyl mimetics as signaling modulators and potential antitumor agents. *Bioorg. Med. Chem.* **2000**, *2* (2), 189–210. (b) Carboxy-based phosphate mimics have also been reviewed: Burke, T. R., Jr.; Gao, Y.; Yao, Z.-J.; Voigt, J.; Luo, J.; Yang, D. Potent non phosphate-containing Grb2 SH2 domain inhibitors. *Pept. Sci.* **1999**, *36*, 49–52. (c) A hydroxymalonate-based phosphate mimic has been described: Shah, A.; Miller, M. J.; Font, J. L.; Ream, J. E.; Walker, M. C.; Sikorski, J. A. New aromatic inhibitors of EPSP synthase incorporating hydroxymalonates as novel 3-phosphate replacements. *Bioorg. Med. Chem.* **1997**, *5* (2), 323–334. Cleary, D. G.; Ream, J. E.; Snyder, K. R.; Sikorski, J. A. New EPSP synthase inhibitors: synthesis and evaluation of an aromatic tetrahedral intermediate mimic containing a 3-malonate ether as a 3-phosphate surrogate. *Bioorg. Med. Chem.* **1995**, *3* (12), 1685–1692. Miller, M. J.; Braccolino, D. S.; Cleary, D. G.; Ream, J. E.; Walker, M. C.; Sikorski, J. A. EPSP synthase inhibitors design. IV. New aromatic substrate analogs and symmetrical inhibitors containing novel 3-phosphate mimics. *Bioorg. Med. Chem. Lett.* **1994**, *4* (21), 2605–2608. Sikorski, J. A.; Miller, M. J.; Braccolino, D. S.; Cleary, D. G.; Corey, S. D.; Font, J. L.; Gruys, K. J.; Han, C. Y.; Lin, K. C. EPSP synthase: the design and synthesis of bisubstrate inhibitors incorporating novel 3-phosphate mimics. *Phosphorus, Sulfur Silicon Relat. Elem.* **1993**, *76* (1–4), 375–378.
- (22) Gao, Y.; Wu, L.; Luo, J. H.; Guo, R.; Yang, D.; Zhang, Z.-Y.; Burke, T. R., Jr. Examination of novel non-phosphorus-containing phosphotyrosyl mimetics against protein-tyrosine phosphatase-1B and demonstration of differential affinities toward Grb2 SH2 domains. *Bioorg. Med. Chem. Lett.* **2000**, *10* (9), 923–927. Burke, T. R., Jr.; Gao, Y.; Yao, Z.-J.; Voigt, J.; Luo, J.; Yang, D. Potent non phosphate-containing Grb2 SH2 domain inhibitors. *Pept. Sci.* **1999**, *36*, 49–52. Burke, T. R., Jr.; Luo, J.; Yao, Z.-J.; Gao, Y.; Zhao, H.; Milne, G. W. A.; Guo, R.; Voigt, J. H.; King, C. R.; Yang, D. Monocarboxylic-based phosphotyrosyl mimetics in the design of Grb2 SH2 domain inhibitors. *Bioorg. Med. Chem. Lett.* **1999**, *9* (3), 347–352 and references therein.
- (23) Before we had a chance to report about this work, T. Burke published on the synthesis of a high-affinity ligand for Grb2 SH2 incorporating a malonate moiety as replacement for the phosphate: Gao, Y.; Luo, J.; Yao, Z.-J.; Guo, R.; Zou, H.; Kelley, J.; Voigt, J. H.; Yang, D.; Burke, T. R., Jr. Inhibition of Grb2 SH2 Domain Binding by Non-Phosphate-Containing Ligands. 2. 4-(2-Malonyl)phenylalanine as a Potent Phosphotyrosyl Mimetic. *J. Med. Chem.* **2000**, *43* (5), 911–920.
- (24) Lesuisse, D. SAR by Crystallography: A New Approach Combining Screening and Rational Drug Design. Application to the Discovery of Nanomolar Src SH2 Binders. Presented at the 8th Meeting of the French American Chemical Society, June 4–8, 2000, Sonoma County.
- (25) Browning, A. F.; Greeves, N. Palladium-catalyzed carbon-carbon bond formation. *Transition Met. Org. Synth.* **1997**, 35–64.
- (26) Shuker, S. B.; Hadjuk, P. J.; Meadows, R. P.; Fesik, S. W. Discovering high-affinity ligands for proteins: SAR by NMR. *Science* **1996**, *274*, 1531–1534.
- (27) Hajduk, P. J.; Zhou, M.-M.; Fesik, S. W. NMR-Based Discovery of Phosphotyrosine Mimetics That Bind to the Lck SH2 Domain. *Bioorg. Med. Chem. Lett.* **1999**, *9* (3), 2403–2406.
- (28) Nienaber, V. L.; Richardson, P. L.; Klighofer, V.; Bouska, J. J.; Giranda, V. L.; Greer, J. Discovering novel ligands for macromolecules using X-ray crystallographic screening. *Nat. Biotechnol.* **2000**, *28*, 1105–1106.
- (29) Lynch, B. A.; Loiacono, K. A.; Lai Tiong, C.; Adams, S. E.; Mac Neil, I. A. A fluorescence polarization based Src-SH2 binding assay. *Anal. Biochem.* **1997**, *247*, 77–82.
- (30) Kabsch, W. Automatic processing of rotation diffraction data from crystals of initially unknown symmetry and cell constants. *J. Appl. Crystallogr.* **1993**, *26* (6), 795–800.
- (31) Brunger, A. T. Slow-cooling protocols for crystallographic refinement by simulated annealing. *Acta Crystallogr., Sect. A: Found. Crystallogr.* **1990**, *A46* (1), 46–57.
- (32) Hatada, M. Private communication.
- (33) Oldfield, T. J.; Hubbard, R. E. Analysis of C alpha geometry in protein structures. *Proteins* **1994**, *18* (4), 324–337.
- (34) Kabsch, W. Evaluation of single-crystal x-ray diffraction data from a position-sensitive detector. *J. Appl. Crystallogr.* **1988**, *21* (6), 916–924.
- (35) Ladbury, J. E.; Lemmon, M. A.; Zhou, M.; Green, J.; Botfield, M. C.; Schlessinger, J. Measurement of the binding of tyrosyl phosphopeptides to SH2 domains: a reappraisal. *PNAS* **1995**, *92* (8), 3199–3203.
- (36) Lagrange, J. *J. Pharm. Belg.* **1962**, *17*, 3.

JM010927P